© 2022. Published by The Company of Biologists Ltd | Journal of Cell Science (2022) 135, jcs259450. doi:10.1242/jcs.259450

RESEARCH ARTICLE

Oligopeptide transporter Slc15A modulates macropinocytosis in *Dictyostelium* by maintaining intracellular nutrient status

Yiwei Zhang[1,2,*], Hui Tu[1,2,*], Yazhou Hao[1,2], Dong Li[1,3], Yihong Yang[1], Ye Yuan[1,2], Zhonglong Guo[4], Lei Li[4], Haibin Wang[1,‡] and Huaqing Cai[1,2,‡]

ABSTRACT

Macropinocytosis mediates non-selective bulk uptake of extracellular fluid. It is the major route by which axenic *Dictyostelium* cells obtain nutrients and has emerged as a nutrient-scavenging pathway in mammalian cells. How environmental and cellular nutrient status modulates macropinocytic activity is not well understood. By developing a high-content imaging-based genetic screen in *Dictyostelium discoideum* we identified Slc15A, an oligopeptide transporter located at the plasma membrane and early macropinosome, as a novel macropinocytosis regulator. We show that deletion of *slc15A* but not two other related *slc15* genes, leads to reduced macropinocytosis, reduced cell growth and aberrantly increased autophagy in cells grown in nutrient-rich medium. Expression of Slc15A protein or supplying cells with free amino acids rescues these defects. In contrast, expression of transport-defective Slc15A or supplying cells with amino acids in their di-peptide forms fails to rescue these defects. Therefore, Slc15A modulates the level of macropinocytosis by maintaining the intracellular availability of key amino acids through extraction of oligopeptides from the early macropinocytic pathway. We propose that Slc15A constitutes part of a positive feedback mechanism coupling cellular nutrient status and macropinocytosis.

This article has an associated First Person interview with the first authors of the paper.

KEY WORDS: *Dictyostelium*, Macropinocytosis, Nutrient status, Oligopeptide transporter

INTRODUCTION

Macropinocytosis is a cellular process that mediates non-selective bulk uptake of extracellular fluid. Studies in the model system *Dictyostelium discoideum* and immune cells have greatly facilitated our understanding of the cellular mechanisms that govern macropinocytosis (King and Kay, 2019). During this process, sheet-like extensions of the plasma membrane give rise to micrometer-sized vesicles called macropinosomes. In the initial step of macropinosome formation, membrane extensions evolve into macropinocytic cups, which are organized around patches of active Ras, Rac and phosphatidylinositol (3,4,5)-trisphosphate (PIP_3), with actin-polymerizing activities that are driven, respectively, by the SCAR/WAVE complex and formin proteins at the periphery and base of the patches (Buckley et al., 2020; Fujii et al., 2013; Junemann et al., 2016; Mylvaganam et al., 2021; Veltman et al., 2016; Yoshida et al., 2009). A 'tent-pole mechanism', in which filopodia-like F-actin extensions twist to constrict the forming macropinosomes, has also been proposed (Condon et al., 2018). Once formed, macropinosomes can either recycle to the cell surface or mature by trafficking through the endolysosomal system where their contents are digested and extracted (Buckley and King, 2017; Donaldson, 2019; Freeman et al., 2020).

Macropinocytosis was originally recognized as a means for cells of the innate immune system, such as macrophages and dendritic cells, to survey environmental antigens for presentation to B cells and T cells (Lin et al., 2020; Norbury et al., 1995; Sallusto et al., 1995). More recently, studies in mammalian and *Dictyostelium* cells have uncovered an important metabolic function of macropinocytosis (Charpentier et al., 2020; King and Kay, 2019; Palm, 2019). Various types of cancer cells exploit macropinocytosis to survive in nutrient-poor environments by ingesting extracellular macromolecules and breaking them down in the lysosome to fuel cell growth (Commisso et al., 2013; Kim et al., 2018; Palm et al., 2015, 2017; Ramirez et al., 2019; Wyant et al., 2017; Yao et al., 2019). Axenic laboratory strains of *Dictyostelium* utilize macropinocytosis to obtain nutrients, including glucose and amino acids, from liquid medium (Bloomfield et al., 2015; Williams and Kay, 2018). These strains were isolated by selecting cells that performed macropinocytosis at a high rate in liquid culture. The mutations that allow axenic growth have been mapped to three separate loci, one of which is a gene encoding the RasGAP neurofibromin (*axeB; Nf1* in mammals) (Bloomfield et al., 2015; Clarke and Kayman, 1987).

As a means of acquiring nutrients, the extent of macropinocytosis is intrinsically connected to the nutritional status of the cell. In pancreatic ductal adenocarcinoma cells (PDACs), glutamine deprivation or restriction of extracellular proteins as the source of essential amino acids induces macropinocytosis (King et al., 2020; Lee et al., 2019). Amino acid shortage has also been shown to promote macropinocytosis in human placental trophoblasts (Shao et al., 2021). In axenic *Dictyostelium* cells, the presence of bacteria as a nutrient source promotes phagocytosis and suppresses macropinocytosis, whereas switching the feeding strategy to liquid medium prominently increases the rate of macropinocytosis (Kayman and Clarke, 1983; Williams and Kay, 2018). Although these observations demonstrate that cells can calibrate their macropinocytic activity according to changes in nutrient conditions, how this is achieved in cells and what the full complement of regulators are remain to be elucidated.

[1]National Laboratory of Biomacromolecules, Institute of Biophysics, Chinese Academy of Sciences, Beijing 100101, China. [2]College of Life Sciences, University of Chinese Academy of Sciences, Beijing 100049, China. [3]Division of Life Sciences and Medicine, University of Science and Technology of China, Hefei 230027, China. [4]State Key Laboratory of Protein and Plant Gene Research, School of Life Sciences and School of Advanced Agricultural Sciences, Peking University, Beijing 100871, China.
*These authors contributed equally to this work

‡Authors for correspondence (huaqingcai@ibp.ac.cn; wanghaibin@ibp.ac.cn)

Y.Z., 0000-0001-8994-1808; H.T., 0000-0002-1898-2685; Y.Y., 0000-0001-9564-9563; Z.G., 0000-0002-3879-8738; H.C., 0000-0001-8434-6639

Handling Editor: Mahak Sharma
Received 9 October 2021; Accepted 2 March 2022

Journal of Cell Science (2022) 135, jcs259450. doi:10.1242/jcs.259450

We developed a forward genetic screen in *Dictyostelium* to seek novel macropinocytosis regulators. In this study, we further characterized one of the genes isolated from the screening, which encodes an oligopeptide transporter we named Slc15A. We show that, opposite to the strategy of mammalian cells, Slc15A constitutes part of a positive feedback mechanism coupling cellular nutrient status and macropinocytosis. Furthermore, Slc15A modulates the level of macropinocytosis by acting in the early macropinocytic pathway instead of the lysosome where nutrient extraction is thought to take place in canonical models. Our results demonstrate that macropinocytosis and its regulation are far more sophisticated than we currently understand.

RESULTS

Screening for macropinocytosis regulators identified Slc15A

To screen for macropinocytosis regulators, we generated a pool of restriction enzyme-mediated insertion (REMI) mutants in the axenic *Dictyostelium* strain Ax2. Individual mutant clones were incubated with 70 kDa tetramethylrhodamine isothiocyanate dextran (TRITC dextran, hereafter referred to as TD) in liquid growth medium and then subjected to image-based high-content analysis (Fig. 1A). Cell boundaries and intracellular vesicles containing TD were identified in the digital phase-contrast channel and fluorescent channel, respectively (Fig. 1A). The ratio of the total intensity of TD spots to the total cell area was used to quantify the activity of macropinocytosis. In addition to Ax2 cells, cells deleted of class-1 phosphoinositide 3-kinases (PI3Ks) were used as controls. Consistent with previous reports (Hoeller et al., 2013), cells deleted for genes encoding PI3Ks exhibited significantly reduced macropinocytosis under these experimental conditions (Fig. 1B).

From the screen, we obtained a series of macropinocytosis mutants (Fig. 1C). This report focuses on the gene we named *slc15A* (dictyBase gene ID: DDB_G0272550), which encodes a protein homologous to the mammalian solute carrier family 15 proteins (Fig. S1A). SLC15 proteins are proton-coupled oligopeptide transporters (POTs) mediating the cellular uptake of a wide range of di- and tri-peptides and peptide-like drugs (Daniel et al., 2006; Smith et al., 2013). Phylogenetic analysis revealed that the SLC15 family in eukaryotes constitutes two clades, and *Dictyostelium* Slc15A is closely related to the mammalian SLC15A1 and SLC15A2 (Fig. S1A). Sequence alignment showed that Slc15A shares 45–46% similarity to human SLC15A1 and SLC15A2 (Fig. S1B).

The REMI insertion site was identified at position 795 of the *slc15A* genomic locus (numbered from the ATG translation start site, Fig. S1B). To confirm whether this insertion is, indeed, responsible for the observed phenotype, we generated *slc15A* knockout (*slc15A*$^-$) cell line in Ax2 (Fig. S2A). The knockout cells exhibited similar phenotypes as the REMI mutant. When incubated with TD, substantially fewer and less bright TD-containing vesicles were observed in *slc15A*$^-$ cells compared to Ax2 cells (Fig. 2A,B). Similarly, the macropinocytic uptake of 70 kDa fluorescein isothiocyanate-dextran (FITC dextran, FD) was significantly impaired in *slc15A*$^-$ cells (Fig. S2B). Quantification of macropinocytosis over time corroborated these findings. The rate of macropinocytosis and the steady-state plateau were reduced by ∼50% in *slc15A*$^-$ cells compared to that in control (Fig. 2C). In contrast, fluid-phase exocytosis was not affected (Fig. 2D). Furthermore, the macropinocytosis defects associated with *slc15A* deletion could be fully rescued by expression of GFP- or RFP-tagged Slc15A (Fig. 2A-C and Fig. S2B). We also generated a *slc15A*$^-$ cell line in the non-axenic *Dictyostelium* strain DdB (Fig. S2C). Macropinocytic activity was considerably lower in DdB compared to Ax2 (Fig. S2D), and deletion of *slc15A* further decreased this activity (Fig. 2E,F). These experiments confirm that Slc15A is a novel regulator of macropinocytosis.

Slc15A is specifically required for macropinocytosis regulation

To begin elucidating the function of Slc15A, we examined the distribution and dynamics of several macropinocytic marker proteins in Ax2 and *slc15A*$^-$ cells. Rab5A, Rab7A, the V-ATPase subunit VatB, the PIP_3/$PI(3,4)P_2$ sensor PHcrac, the $PI(3,4)P_2$ sensor TAPP1 or the PI(3)P sensor 2×FYVE were fused with GFP or RFP and used to mark macropinosomes at different stages (Buckley and King, 2017; Dormann et al., 2004; Egami et al., 2014; Maekawa et al., 2014; Rupper et al., 2001; Swanson, 2014). We observed that the overall organization of the macropinocytic pathway appeared unaffected by *slc15A* deletion. Marker proteins

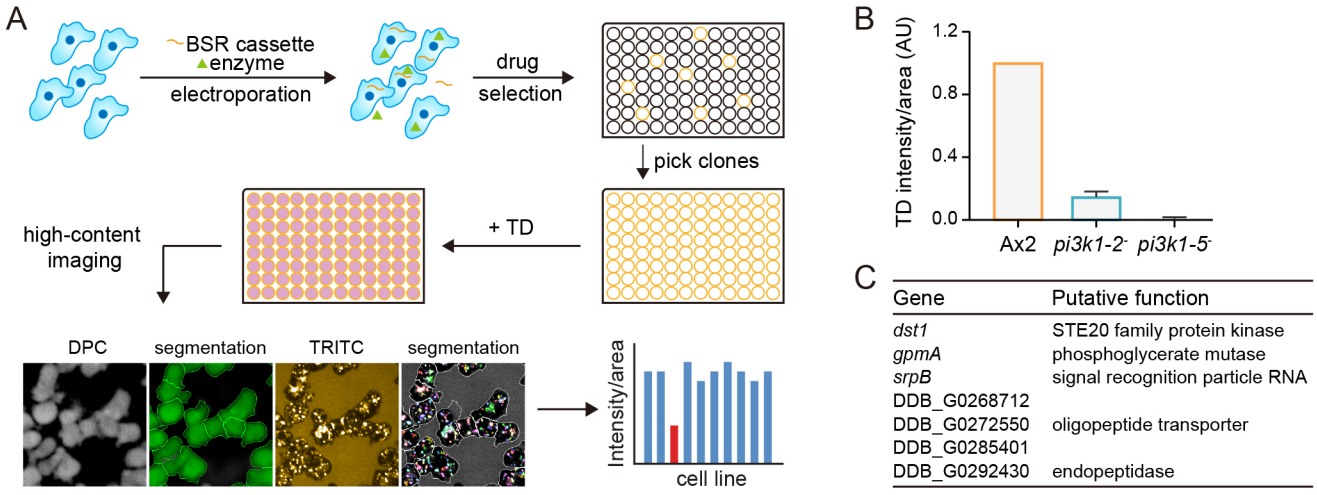

Gene	Putative function
dst1	STE20 family protein kinase
gpmA	phosphoglycerate mutase
srpB	signal recognition particle RNA
DDB_G0268712	
DDB_G0272550	oligopeptide transporter
DDB_G0285401	
DDB_G0292430	endopeptidase

Fig. 1. Screening for macropinocytosis regulators. (A) Schematic of the genetic screen. Mutant clones were generated by REMI, seeded in 96-well plates in growth medium and incubated with TD. Images were captured in the digital phase contrast (DPC) and TRITC channels using a high-content screening system. The ratio of the total intensity of TD spots to the sum of cell area was used to quantitatively measure macropinocytosis. (B) Cells of the Ax2 strain deleted for PI3K1 and 2 (*pi3k1-2* null) or PI3K1-5 (*pi3k1-5* null) were analyzed for TD uptake by using the screening system. Data are from three independent experiments; mean ±s.d. (C) List of mutants obtained from the screen.

Journal of Cell Science

Journal of Cell Science (2022) 135, jcs259450. doi:10.1242/jcs.259450

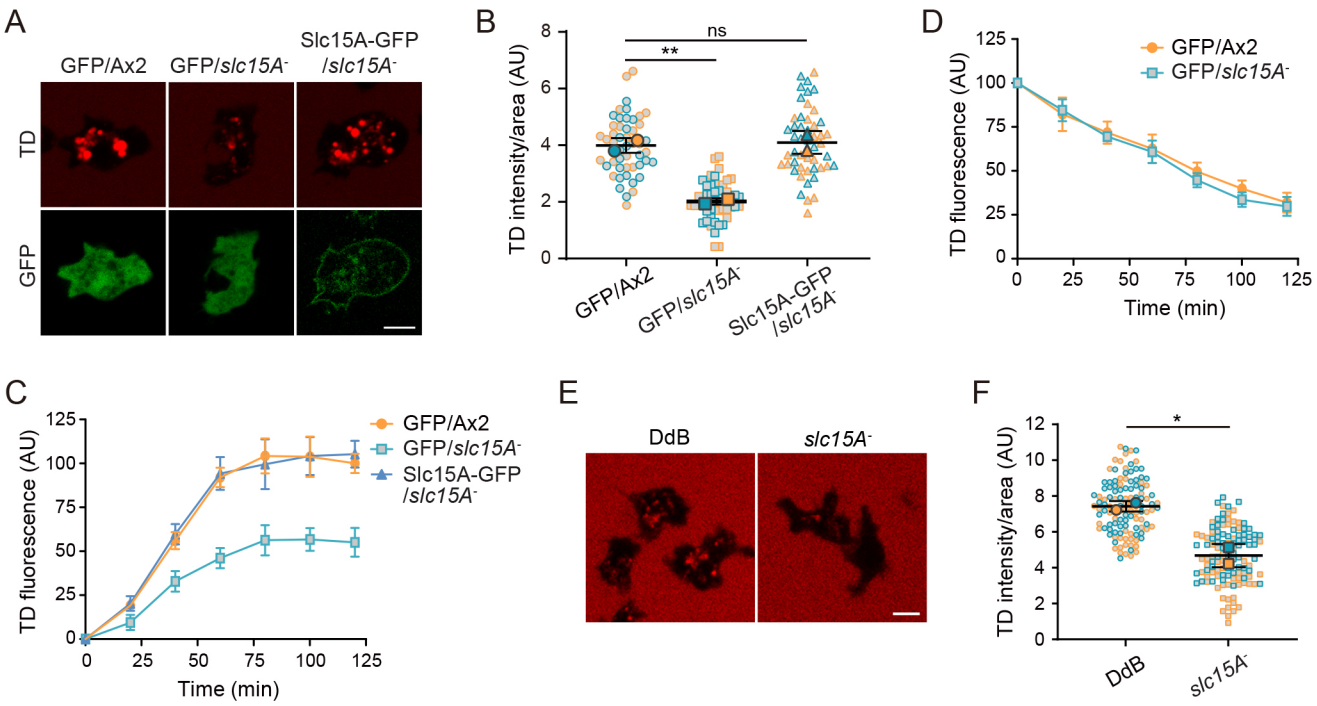

Fig. 2. Slc15A is involved in the regulation of macropinocytosis. (A,B) Confocal images and quantification of TD uptake in Ax2 strain wild-type expressing GFP (GFP/Ax2) and *slc15A*$^-$ cells expressing GFP or Slc15A-GFP (*GFP*/*slc15A*$^-$ or Slc15A-GFP/*slc15A*$^-$, respectively). Data are from two independent experiments with at least 20 cells quantified per experiment (each experiment is shown in a different color); mean±s.d. (C,D) Quantification of TD macropinocytosis (C) and exocytosis (D) by fluorimetric analysis. Data are from four independent experiments; mean±s.d. (E,F) Confocal images and quantification of TD uptake in DdB and *slc15A*$^-$ cells. Data are from two independent experiments with at least 50 cells quantified per experiment (each experiment is shown in a different color); mean ±s.d. Statistical significance was determined by one-way ANOVA with Dunnett post-test (B) and two-tailed unpaired *t*-test (F). Scale bars: 5 µm.

exhibited similar localization in Ax2 and *slc15A*$^-$ cells (Fig. 3A), and the sequential accumulation of PIP_3, $PI(3,4)P_2$, and PI(3)P proceeded with similar kinetics (Fig. 3B and Fig. S3). Measurement of macropinosome acidification also did not reveal any apparent defect in *slc15A*$^-$ cells (Fig. S4). However, time-lapse imaging and quantification by using PHcrac-GFP to mark macropinocytic cups and newly internalized macropinosomes revealed a significant reduction in the rate of macropinosome formation in *slc15A*$^-$ cells. Despite the production of similar-sized vesicles, the number of macropinosomes successfully generated per cell per minute was reduced by ∼40% in *slc15A*$^-$ compared to Ax2 cells (Fig. 4A-C, Movie 1). In many instances, macropinocytic cups formed in *slc15A*$^-$ cells collapsed and receded to the plasma membrane without vesicle formation (Fig. 4A).

As macropinocytosis is the main pathway by which axenic cells obtain nutrients from liquid medium (Hacker et al., 1997), its defect often manifests as slow cell growth. Indeed, the generation time in shaken suspension increased from ∼8 h for Ax2 cells to ∼15 h for *slc15A*$^-$ cells (Fig. 4D). Expression of Slc15A-GFP rescued this defect (Fig. 4D). Lack of nutrient uptake has also been shown to upregulate autophagy. Imaging the autophagy marker Atg8a tagged to GFP (GFP-Atg8a) (King et al., 2011) revealed that, although non-nutrient development buffer (DB) induced autophagy to a similar extent in Ax2 and *slc15A*$^-$ cells, the latter showed significantly increased autophagy in the commonly used HL5 growth medium (Fig. 4E,F; Movies 2 and 3). The increase of Atg8a structures in *slc15A*$^-$ cells was not caused by a block of autophagy flux (Fig. S5). Therefore, *slc15A* deletion likely impairs macropinocytosis-mediated nutrient uptake, resulting in reduced cell growth and aberrantly increased autophagy in cells cultured in nutrient-rich medium.

In addition to liquid medium, *Dictyostelium* cells could utilize bacteria as the nutrient source through phagocytosis. We investigated whether Slc15A is involved in the regulation of phagocytosis. When plated on bacterial (*Klebsiella aerogenes*) lawns, the plaque growth of *slc15A*$^-$ cells was indistinguishable from that of Ax2 cells, indicating that bacterial uptake and digestion were not affected (Fig. S2A). Quantifying bacteria phagocytosis by using flow cytometry analysis and assaying the proteolytic activity of bacteria-containing phagosomes confirmed this conclusion (Fig. 4G,H). Together, these experiments indicate that Slc15A is specifically involved in the regulation of macropinocytic, but not phagocytic growth.

Slc15A promotes macropinocytosis by maintaining intracellular availability of amino acids

To determine whether Slc15A modulates macropinocytosis through its putative function as an oligopeptide transporter, we generated a Slc15A variant bearing mutations (Slc15A^{mut}-GFP) in the two conserved residues R68 and E438 (Fig. S1B). The corresponding mutations R57H and E595R in human SLC15A2 and SLC15A1, respectively, have previously shown to abolish transport function (Terada et al., 2004; Xu et al., 2009). Although Slc15A^{mut}-GFP was expressed at a level similar to its WT counterpart, it failed to rescue the TD uptake and cell growth defects (Fig. 5A-C). This suggests that the oligopeptide transport activity is required for Slc15A to regulate macropinocytosis.

The standard HL5 medium contains amino acids, peptides and proteins derived from peptone and yeast extract. We therefore speculated that deletion of *slc15A* causes reduced peptide import from HL5 and, thus, a lack of amino acid-nutrients in cells, which in

Journal of Cell Science (2022) 135, jcs259450. doi:10.1242/jcs.259450

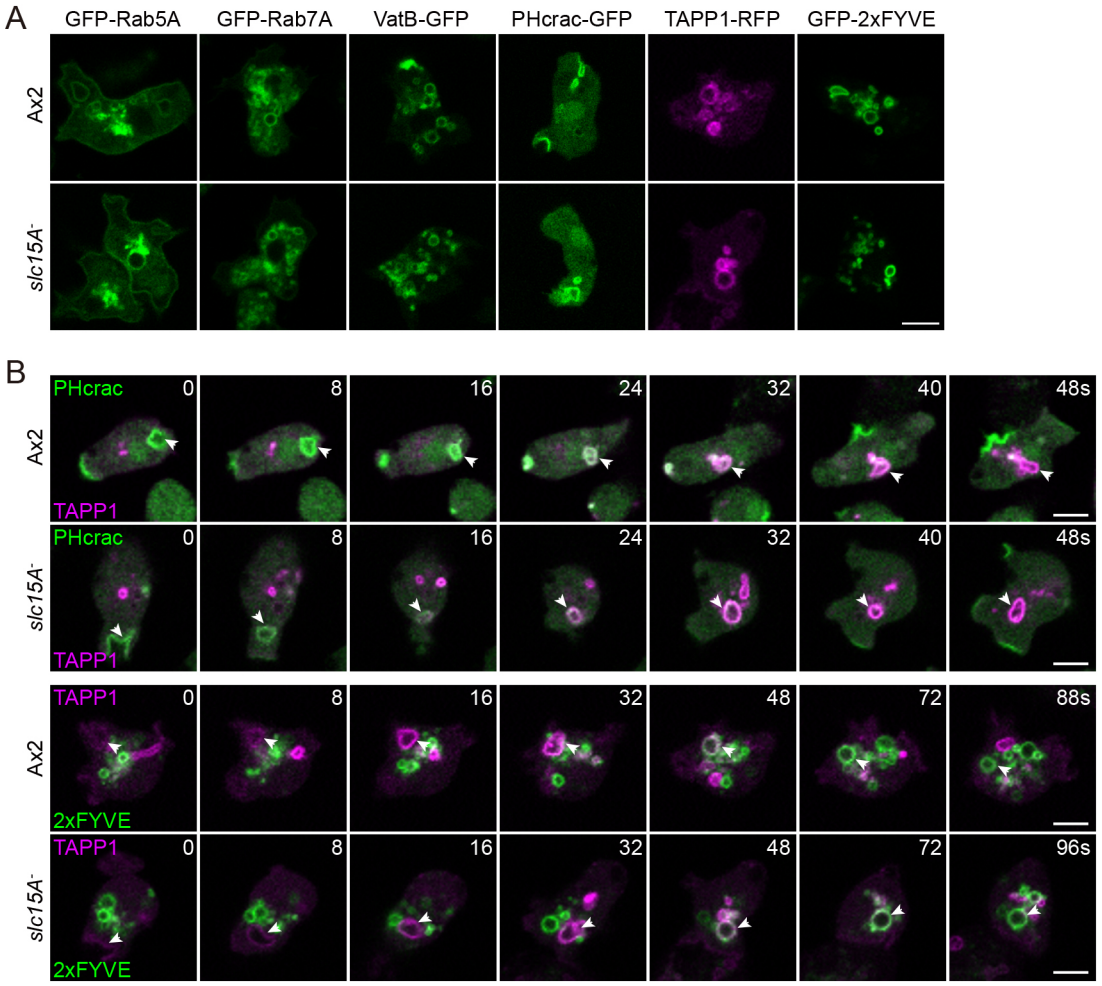

Fig. 3. Localization of macropinocytic marker proteins in Ax2 strain wild-type **and *slc15A* deletion cells.** (A) Confocal images of the indicated marker proteins in Ax2 and *slc15A*$^{-}$ cells. (B) Top: Time-lapse images showing the sequential accumulation of PHcrac-GFP and TAPP1-RFP in Ax2 and *slc15A*$^{-}$ cells. Bottom: Time-lapse images showing the sequential accumulation of TAPP1-RFP and GFP-2×FYVE in Ax2 and *slc15A*$^{-}$ cells. Scale bars: 5 µm.

turn might downregulate macropinocytosis. Were this true, providing *slc15A*$^{-}$ cells with free amino acids, which bypass the need for peptide transport, should rescue the macropinocytosis defect. To test this, we replaced HL5 with SIH medium, a synthetic medium containing a defined composition of free amino acids sufficient to sustain cell growth. Growing *slc15A*$^{-}$ cells in SIH medium fully rescued the macropinocytosis defect (Fig. 5D,E and Fig. S6), and cell growth and autophagy regulation were also restored (Fig. 5F,G; Movies 2 and 3). These experiments support our hypothesis that reduced amino acid availability underlies the macropinocytosis defect of *slc15A*$^{-}$ cells.

To determine whether specific amino acids within the SIH medium are crucial for the rescuing effect, we subjected *slc15A*$^{-}$ cells to SIH medium lacking arginine, glutamate or lysine, as these three amino acids had been shown to be needed for the upregulation of macropinocytosis when the feeding strategy was switched from growth on bacteria to liquid medium (Williams and Kay, 2018). Intriguingly, removing arginine (SIH-R) or lysine (SIH-K), but not glutamate (SIH-E), abolished the ability of SIH medium to rescue the macropinocytosis defect caused by *slc15A* deletion (Fig. 6A,B). Ax2 cells cultured in SIH-R or SIH-K also exhibited reduced macropinocytosis (Fig. 6A,B). These results indicate that *slc15A* deletion likely causes reduced availability of key amino acids, including arginine and lysine.

To further test whether Slc15A-mediated oligopeptide transport contributes to the intracellular pool of arginine and lysine, we subjected cells to medium containing synthesized dipeptide of arginine (R-R) or lysine (K-K). Supplementing R-R or K-K restored the macropinocytosis ability of Ax2 cells grown in SIH-R or SIH-K. However, it failed to do so for *slc15A*$^{-}$ cells, confirming that the knockout cells are defective in dipeptide utilization (Fig. 6C,D). These experiments collectively indicate that Slc15A promotes macropinocytosis by functioning as an oligopeptide transporter to maintain the intracellular availability of key amino acids.

Slc15A functions in the early macropinocytic pathway

Extracellular proteins taken up by macropinocytosis are thought to be delivered to the lysosomes, degraded into amino acids, and then exported to the cytosol to fuel metabolism (Verdon et al., 2017; Wyant et al., 2017). However, we noticed that Slc15A did not appear to localize to lysosomal vesicles when expressed from extrachromosomal plasmids. To determine the localization more accurately, we generated Slc15A-GFP and Slc15A-RFP knock-in (KI) cells (Fig. S2E). We found that Slc15A localized to the plasma membrane in these cells and, when the membrane deformed to produce macropinosomes, remained associated with newly generated macropinosomes (Fig. 7A,B). Imaging Slc15A together with TAPP1 and 2×FYVE revealed that Slc15A and TAPP1

Journal of Cell Science (2022) 135, jcs259450. doi:10.1242/jcs.259450

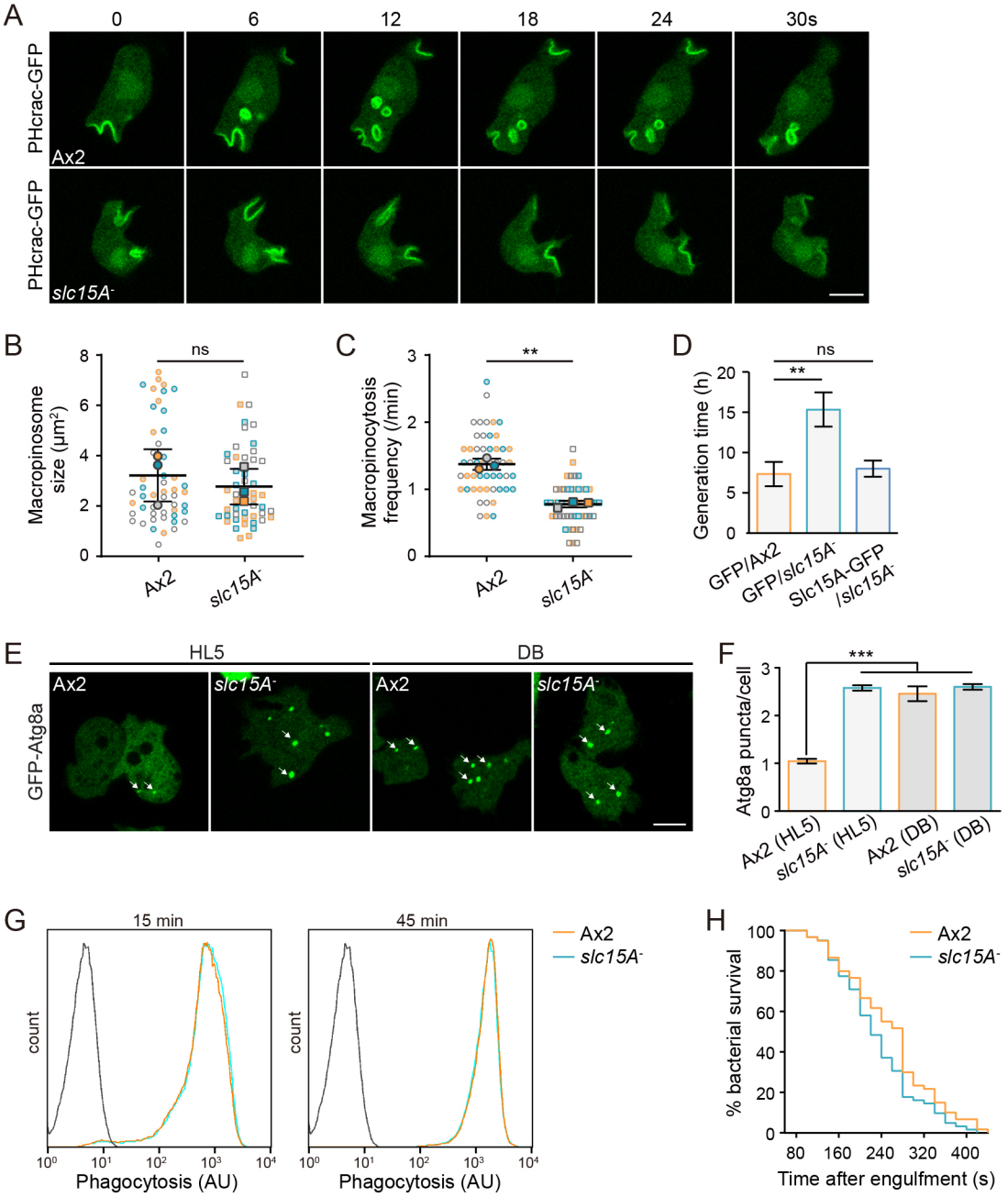

Fig. 4. Macropinocytosis is specifically impaired in *slc15A* deletion cells. (A) Time-lapse images of PHcrac-GFP in Ax2 strain wild-type and *slc15A*$^{-}$ cells. (B,C) Plotted is the size of newly enclosed macropinosomes labeled by PHcrac-GFP and rate of macropinosome formation. Data are from three independent experiments with at least 15 cells quantified per experiment (each experiment is shown in a different color); mean±s.d. (D) Cell growth in HL5 medium measured by generation time. Data are from three independent experiments; mean±s.d. (E) Confocal images of GFP-Atg8a in cells cultured in HL5 or non-nutrient DB for 1 h. (F) Plotted is the average number of Atg8a puncta per cell. Data are from three independent experiments with at least 30 cells quantified per experiment; mean ±s.d. (G) Quantification of bacterial phagocytosis. Cells were incubated with mCherry-expressing *E. coli* for the indicated time points and phagocytosis was measured by flow cytometry. The black lines show the background fluorescence. (H) Quantification of bacterial survival. Cells were incubated with GFP-expressing *E. coli*. The Kaplan-Meyer graph was based on the persistence of bacterial GFP-fluorescence within cells after phagocytosis. Per cell line, 60 bacteria were followed. Statistical significance was determined by two-tailed unpaired *t*-test (B,C) and one-way ANOVA with Dunnett post-test (D,F). Scale bars: 5 µm.

colocalized on macropinosomes during cup closure and initial trafficking (Fig. 7A, Movie 4); the signal of Slc15A gradually decreased as the macropinosomes moved further into the cells, which was accompanied by the gradual accumulation of 2×FYVE (Fig. 7B). These experiments indicate that Slc15A recycles from the macropinosomes in the early stages of the pathway. In line with this finding, we found little overlap between Slc15A and the lysosomal/post-lysosomal marker LmpA (Sattler et al., 2018) (Fig. S7). Thus, Slc15A likely mediates oligopeptide transport across the plasma membrane or the early macropinosomal membrane but not efflux from the lysosome.

Given that the SLC15 family proteins rely on an electrochemical H^+ gradient for transport activity (Smith et al., 2013; Steel et al., 1997), we examined whether the presence of Slc15A on nascent macropinosomes overlapped with macropinosome acidification. By incubating Slc15A-RFP KI cells with FD, we found that newly

Journal of Cell Science (2022) 135, jcs259450. doi:10.1242/jcs.259450

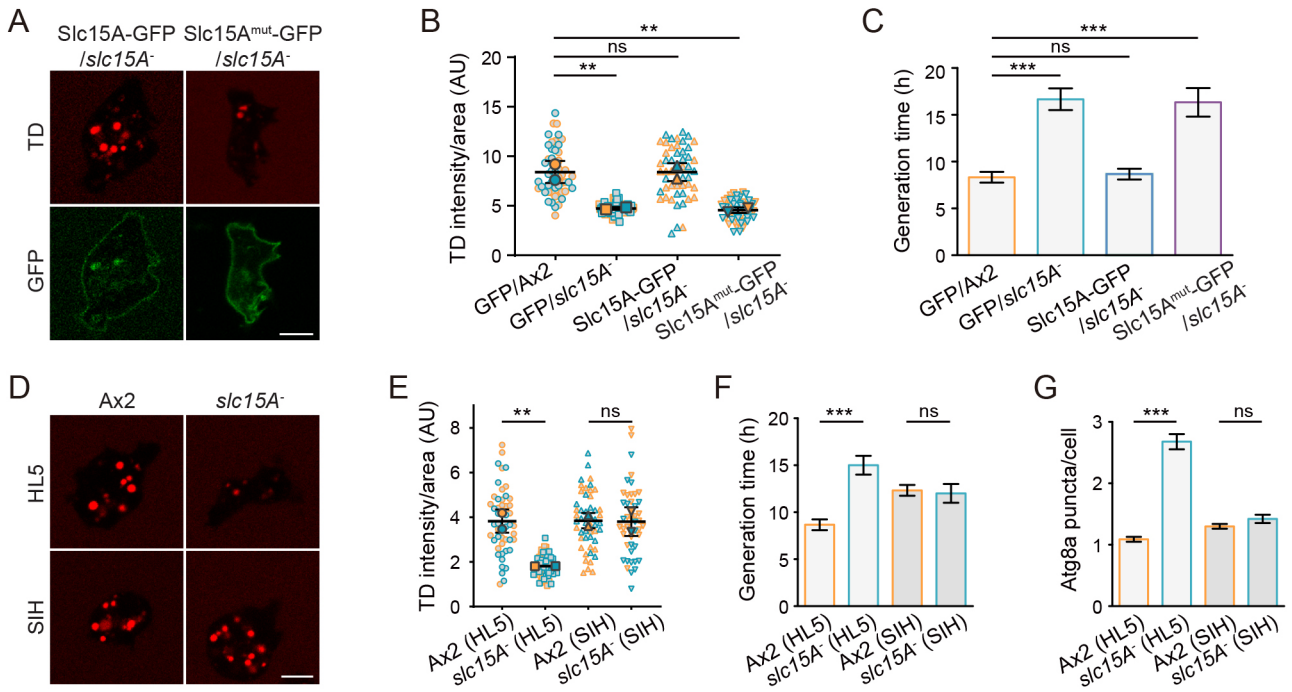

Fig. 5. The oligopeptide transport activity is required for Slc15A to modulate macropinocytosis. (A) Confocal images of TD uptake in *slc15A*$^{-}$ cells expressing Slc15A-GFP or Slc15A^{mut}-GFP bearing R68H and E438R mutations. (B) Quantification of TD uptake in cells transformed with the indicated plasmids. Data are from two independent experiments with at least 20 cells quantified per experiment (each experiment is shown in a different color); mean±s.d. (C) Cell growth in HL5 measured by generation time. Data are from three independent experiments; mean±s.d. (D,E) Confocal images and quantification of TD uptake in Ax2 and *slc15A*$^{-}$ cells grown in HL5 or SIH medium. Data are from two independent experiments with at least 20 cells quantified per experiment (each experiment is shown in a different color); mean±s.d. (F) Cell growth in HL5 or SIH measured by generation time. Data are from three independent experiments; mean±s.d. (G) Plotted is the average number of GFP-Atg8a puncta per cell in cells grown in HL5 or SIH. Data are from three independent experiments with at least 30 cells quantified per experiment. Statistical significance was determined by one-way ANOVA with Dunnett post-test (B,C) and two-tailed unpaired *t*-test (E–G). Scale bars: 5 µm.

generated macropinosomes quickly acquired an acidic environment, indicated by the decrease of FD fluorescence before Slc15A-RFP was evidently recycled (Fig. 7C). Quantification revealed that Slc15A associated with newly internalized macropinosome for 115±31 s (from 15 macropinosomes), whereas macropinosome acidification was initiated almost immediately after cup closure, with a significant drop of pH occurring within 60 s (Fig. S4). Imaging Slc15A together with VatB also revealed that the recruitment of V-ATPase to macropinosomes started before recycling of Slc15A (Fig. 7D). We speculate that the rapid acidification of nascent macropinosomes facilitates the function of Slc15A by providing a steeper proton gradient. However, at this stage we cannot rule out the possibility that Slc15A also functions at the plasma membrane.

DISCUSSION

In summary, we identified Slc15A as a macropinocytosis-specific regulator. We demonstrated that Slc15A is not directly involved in macropinosome formation or maturation; instead, it sustains the macropinocytic activity of cells by mediating oligopeptide transport from growth medium and maintaining the intracellular availability of key amino acids (Fig. 8). The *Dictyostelium* genome encodes two other putative SLC15 family proteins (Fig. S1A). However, these two proteins did not localize to the macropinocytic pathway and their disruption did not affect macropinocytosis (Fig. S8), confirming a unique function of Slc15A.

Characterization of Slc15A allowed us to gain fresh insights into the regulation of macropinocytosis. First, the localization study suggested that Slc15A functions earlier in the macropinocytic pathway. Thus, different from the canonical model, the lysosome is not the only cellular compartment where internalized nutrients are extracted. Although it is not yet feasible to pinpoint precisely where Slc15A-mediated transport occurs, we speculate that nascent macropinosomes are the more probable compartments because their acidic environment could promote the function of Slc15A. The characteristic substrate multispecificity of SLC15 proteins might further facilitate nutrient extraction in the form of oligopeptides before reaching lysosome (Ito et al., 2013). Intriguingly, the defects in *slc15A*$^{-}$ cells were alleviated by feeding cells with free amino acids, which might be delivered to the cell via amino acid transporters. This ability to retrieve nutrients in different forms and, possibly, at different stages along the macropinocytic pathway likely promotes metabolic flexibility. Second, our study indicates that Slc15A contributes to a positive feedback mechanism coupling cellular nutrient status and macropinocytosis (Fig. 8). Disrupting Slc15A, or depleting arginine or lysine from the growth medium all led to reduced macropinocytosis. Taking into account previous studies that analyzed macropinocytosis during a switch in feeding strategy (Williams and Kay, 2018), our experiments convincingly demonstrate that the intracellular availability of key amino acids can, in turn, promote the macropinocytic activity of *Dictyostelium* cells, constituting feedback regulation. Interestingly, seemingly opposite strategies are taken by *Dictyostelium* and mammalian cells to cope with amino acid stress conditions: *Dictyostelium* cells downregulate macropinocytosis, whereas mammalian cells upregulate the process (Lee et al., 2019; Shao et al., 2021). Such a difference might reflect different survival strategies. Starvation in *Dictyostelium* ultimately leads to multicellular development, a process that benefits from reduced macropinocytosis (Veltman et al., 2014, 2016), whereas

Journal of Cell Science (2022) 135, jcs259450. doi:10.1242/jcs.259450

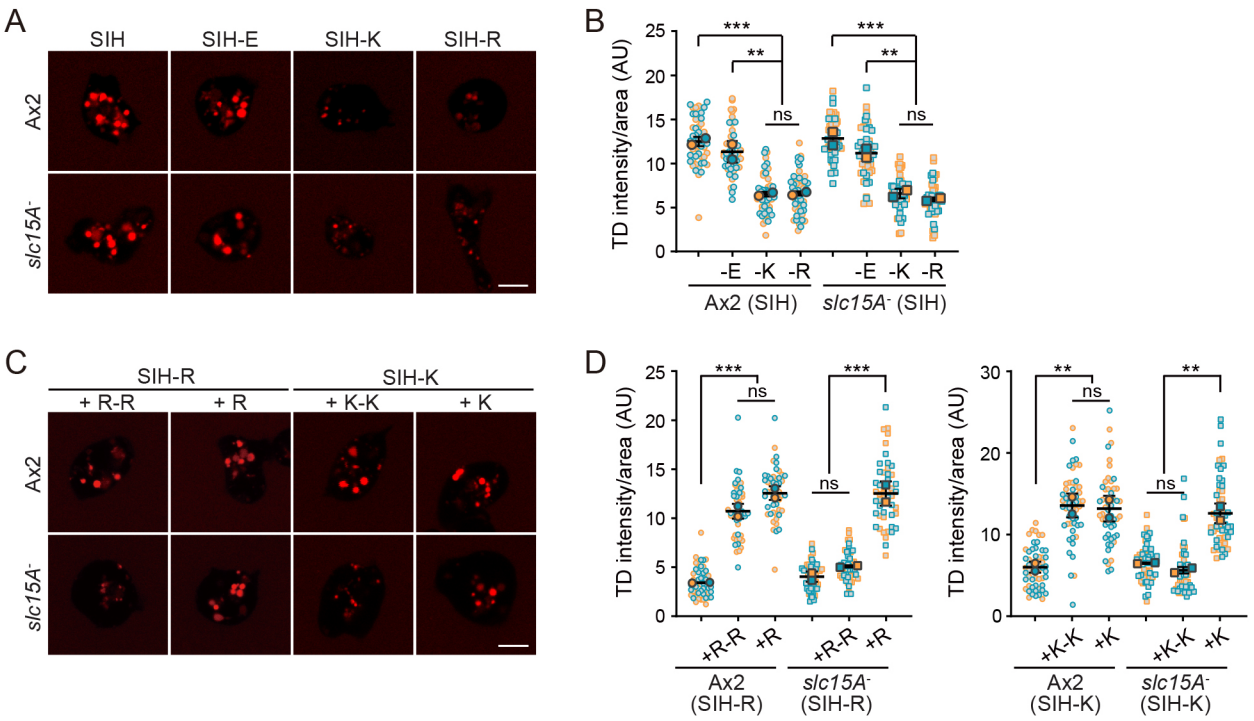

Fig. 6. Slc15A functions to maintain nutrient availability and promote macropinocytosis. (A,B) Confocal images and quantification of TD uptake in Ax2 strain wild-type and *slc15A*$^{-}$ cells cultured in normal SIH or SIH lacking amino acids glutamic acid (E), lysine (K) or arginine (R) – SIH-E, SIH-K or SIH-R, respectively. (C,D) Confocal images and quantification of TD uptake in Ax2 and *slc15A*$^{-}$ cells cultured in SIH-R or SIH-K medium supplemented with the respective single or dipeptide amino acid as indicated. For plots shown in B and D, data are from two independent experiments with at least 20 cells quantified per experiment (each experiment is shown in a different color); mean±s.d. Statistical significance was determined by one-way ANOVA with Tukey post-test. Scale bars: 5 µm.

mammalian cells lacking this alternative route might resort to macropinocytosis upregulation and protein-scavenging instead.

Future studies are needed to elucidate how intracellular nutrient levels are sensed and transduced to regulate macropinocytosis in *Dictyostelium*. In other systems, amino acid-sensing is mediated by activation of the mechanistic target of rapamycin complex 1 (mTORC1) pathway (Wolfson and Sabatini, 2017). It is possible that mTORC1 senses the nutrient stress condition in *slc15A*$^{-}$ cells to downregulate macropinocytosis. However, pharmacological inhibition of mTORC1 or depletion of the mTORC1-specific component Raptor does not affect macropinocytosis in *Dictyostelium* (Rosel et al., 2012; Williams and Kay, 2018), suggesting that the feedback regulation likely involves so-far-unidentified pathways. Additionally, as SLC15 orthologues exist widely in eukaryotes, it will also be of great interest to investigate whether the SLC15 family of proteins is involved in the regulation of macropinocytosis in other species.

MATERIALS AND METHODS

Cell growth

We used cells of the axenic *Dictyostelium* strain Ax2, routinely cultured in HL5 medium (HLF3, Formedium,). Cells carrying expression constructs were maintained in HL5 containing the antibiotics G418 (10–20 µg/ml) or hygromycin (50–100 µg/ml). Development buffer (DB) contained 5 mM Na_2HPO_4, 5 mM KH_2PO_4, 2 mM $MgSO_4$ and 0.2 mM $CaCl_2$. The growth rate was measured by seeding cells at 0.5×10^5/ml and measuring cell density for four consecutive days. DdB cells were used as the non-axenic wild-type strain. Cells of the non-axenic *Dictyostelium* strain DdB were cultured in SorMC buffer (15 mM KH_2PO_4, 2 mM Na_2HPO_4, 50 µM $MgCl_2$ and 50 µM $CaCl_2$, pH 6.0) containing *K. aerogenes* (OD_{600}=2) or grown on *K. aerogenes* lawns as described before (Paschke et al., 2018).

REMI screen

REMI mutants were generated as described previously (Kuspa, 2006; Shaulsky et al., 1996). In brief, a DNA fragment containing a blasticidin resistant cassette (BSR) was digested with BamHI and co-transformed into cells with the DpnII restriction enzyme. Cells were dispensed into 96-well dishes in HL5 medium and blasticidin (10 µg/ml) was added the next day to select mutant clones that had DNA-containing BSR inserted into their genome. Individual mutant clones were seeded in 96-well plates in growth medium, incubated with 70 kDa tetramethylrhodamine isothiocyanate dextran (TRITC dextran, hereafter referred to as TD; Sigma, T1162) for 1 h, and then analyzed using a PerkinElmer Phenix Opera high-content screening system. Images were captured in the digital phase contrast channel and TRITC channel with nine fields per well using a 63× water lens. Image analyses were performed using the built-in Harmony software. For gene identification of REMI mutants, genomic DNA was digested with PsiI and ligated to circularize fragments; inverse PCR was performed using a pair of outward-facing primers located within the BSR sequence as described previously (Keim et al., 2004). The obtained PCR bands were then sequenced to identify the insertion sites.

Molecular biology

To make knockout constructs for *slc15A*, *slc15B* or *slc15C* in Ax2, a BSR cassette (Faix et al., 2004) was inserted into pBlue-Script II SK+ to generate pBlueScript-BSR. Thereafter, 5′ and 3′ arms were PCR-amplified from genomic DNA by using primers listed in Table S1, and cloned upstream and downstream of the BSR cassette, respectively. The resulting disruption cassette was PCR amplified and electroporated into Ax2. Gene disruption was confirmed by resistance to blasticidin (10 µg/ml) and PCR amplification. To make knockout construct for *slc15A* deletion in DdB, 5′ and 3′ arms were PCR amplified with primers listed in Table S1 and cloned upstream and downstream of the NeoR cassette in pDM1082, respectively. Transfection and selection were performed as described before (Paschke et al., 2018). Gene disruption was confirmed by resistance to G418

Journal of Cell Science (2022) 135, jcs259450. doi:10.1242/jcs.259450

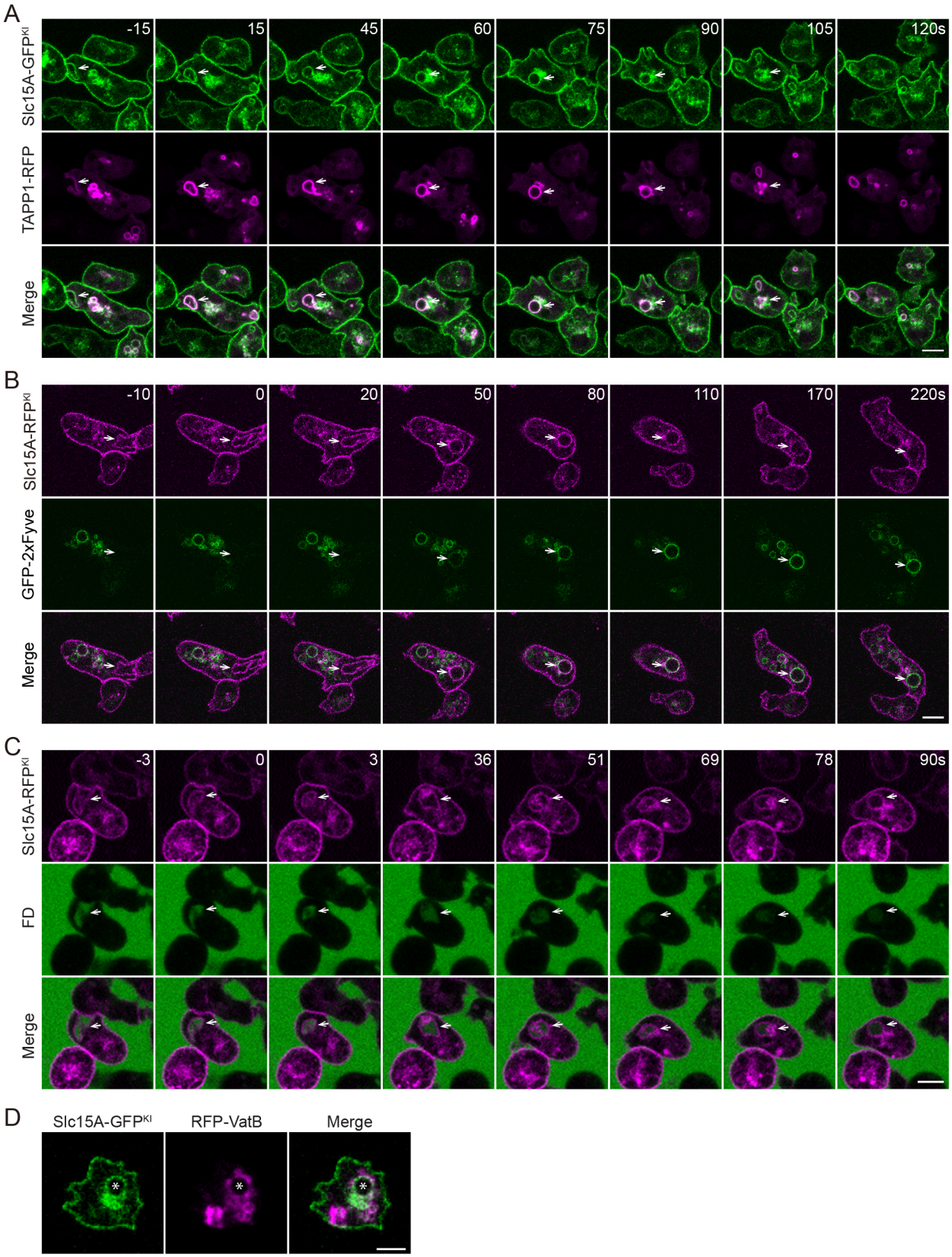

Fig. 7. Slc15A functions in the early macropinocytic pathway. (A) Time-lapse images of Slc15A-GFP^{KI} and TAPP1-RFP in Ax2 strain wild-type cells during macropinocytosis. Arrows indicate a newly generated macropinosome with which Slc15A and TAPP1 associated for ∼100 s. (B) Time-lapse images of Slc15A-RFP^{KI} and GFP-2×FYVE in Ax2 cells during macropinocytosis. Arrows indicate a newly generated macropinosome that had been converted from Slc15A positive to 2×FYVE positive. (C) Time-lapse images of Slc15A-RFP^{KI} in cells incubated with FD. Arrows indicate a newly generated macropinosome that quickly acquired an acidic environment – indicated by the decrease of the fluorescence of FD. (D) Confocal images of Slc15A-GFP^{KI} and RFP-VatB. Asterisks indicate a nascent macropinosome marked by both Slc15A-GFP and RFP-VatB. Scale bars: 5 µm.

Journal of Cell Science (2022) 135, jcs259450. doi:10.1242/jcs.259450

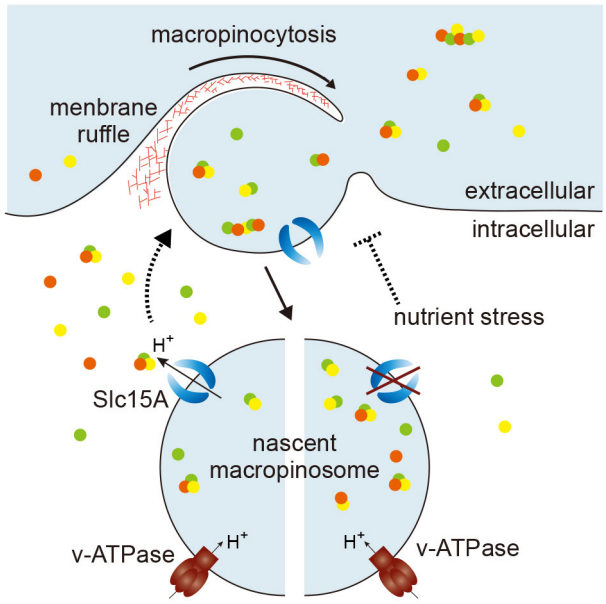

Fig. 8. Working model. Slc15A, a proton-coupled oligopeptide transporter located at the plasma membrane and early macropinosome, mediates oligopeptide transport from growth medium to the cytosol, thereby maintaining the intracellular availability of key amino acids and promoting macropinocytosis via a feedback regulation. Disruption of *slc15A* reduces oligopeptide transport and triggers a nutrient stress condition, which in turn impairs macropinocytosis and leads to defects in cell growth and autophagy regulation. Colored dots indicate amino acids and peptides.

(10 µg/ml) and PCR. Slc15A-GFP knock-in cell was generated by replacing the region of *slc15A* between +1920 and +1922 with a GFP-hygromycin cassette from pDM1355 (Paschke et al., 2018). GFP was replaced with RFP to generate the Slc15A-RFP knock-in cassette. Knock-in clones were selected by hygromycin resistance and confirmed by PCR and western blotting.

To generate constructs expressing GFP- or RFP-fusion proteins, DNA fragments encoding *Dictyostelium* Slc15A, Slc15B, Slc15C, Atg8a, Rab5A, Rab7A, VatB, LmpA or human TAPP1 were PCR-amplified using primers listed in Table S1 and cloned into *Dictyostelium* pDM expression vectors (Veltman et al., 2009) containing a multiple cloning site. To generate construct expressing GFP-2×FYVE, a fragment containing 2×FYVE domain of *C. elegans* EEA1 was released from a *C. elegans* expression vector (Li et al., 2009) and cloned into pDM317. To generate Slc15A$^{R68H/E438R}$-GFP, arginine (R) at position 68 and glutamic acid (E) at position 438 were mutated to histidine (H) and R, respectively. To generate constructs expressing RFP-GFP tagged in tandem to Atg8a (RFP-GFP-Atg8a), *atg8a* was first cloned into pDM449 containing a multiple cloning site; GFP was then PCR amplified from pDM317 using primers listed in Table S1 and inserted in between RFP and Atg8a.

Macropinocytosis and exocytosis assays

Macropinocytosis assay by microscopy imaging was routinely performed by incubating cells with 500 ng/µl TD (Sigma T1162) in HL5 for 1 h. For experiments presented in Fig. 2E, bacterially grown non-axenic cells were adapted in HL5 medium supplemented with 10% fetal bovine serum (Gibco 10091-148) for 24 h before incubating with TD in fresh medium. For experiments presented in Fig. 6A, cells cultured in SIH medium (Formedium) were shifted to SIH-K/R/E for 48 h before measuring macropinocytosis. For experiments presented in Fig. 6C, cells cultured in SIH were shifted to SIH-R or SIH-K for 48 h, followed by the addition of R (87.5 mg/l), R-R dipeptide (87.5 mg/l), K (156 mg/l), or K-K dipeptide (156 mg/l) for 24 h before measuring macropinocytosis. To quantify TD uptake, the medial optical section of cell was imaged using a Zeiss 880 inverted microscope equipped with a 63×/1.4 oil immersion objective. Fluorescence intensity was quantified by ImageJ and normalized to the cell area.

Macropinocytosis dynamics was recorded in Ax2 and *slc15A*$^{-}$ cells expressing PHcrac-GFP by time-lapse imaging. The rate of macropinocytosis was quantified by counting the number of enclosed macropinosomes formed in 5 min. Macropinosome size was determined by measuring the area of newly formed macropinosomes immediately after ruffle closure with the freehand line tool in ImageJ.

Fluorimetric analysis of macropinocytosis and exocytosis was performed as described before (Rivero and Maniak, 2006). For macropinocytosis measurement, cells were shaken at a density of 5×10^6/ml in growth medium, and TD was added to a final concentration of 1 mg/ml. Aliquots of 300 µl of cells were taken at each time point and mixed briefly with Trypan Blue solution (2 mg/ml in 20 mM citrate and 150 mM NaCl, pH 4.5) on ice. Cells were washed once with 1 ml ice-cold Sörensen buffer (14.6 mM KH_2PO_4, 2.0 mM Na_2HPO_4, pH 6.1) and resuspended in 0.5 ml Sörensen buffer. For exocytosis measurement, cells were first incubated with 1 mg/ml TD for 180 min, and were then washed and resuspended in fresh HL5 medium. Aliquots of 300 µl of cells were taken at each time point, washed and resuspended in 0.5 ml ice-cold Sörensen buffer. In both experiments, fluorescence was measured immediately using a Tecan Spark fluorescence spectrophotometer (544-nm excitation and 574-nm emission). Obtained values were normalized to protein content.

Phagocytosis assays

Expression of mCherry or GST-GFP was induced in *E. coli* strain BL21 (DE3) with 0.3 mM isopropyl β-D-1-thiogalactoside at 16°C overnight. Harvested bacteria were washed with Sörensen buffer. For flow cytometry analysis, cells were shaken at a density of 4×10^6/ml in Sörensen buffer, and mCherry-expressing bacteria were added to a final density of 2×10^9/ml. Aliquots of 0.5 ml were taken at each time point. Cells were washed with ice-cold Sörensen buffer containing 5 mM sodium azide and resuspended in Sörensen buffer. The total fluorescence intensity per cell was determined by a BD Biosciences Influx flow cytometer and data were analyzed by FlowJo. For bacteria killing assay, GFP-expressing bacteria were resuspended in HL5 medium to a concentration 2×10^8/ml. 10 µl of bacteria culture in 400 µl HL5 was added into 8-well coverslip chambers before addition of 10^5 cells. Images were acquired every 14 s for a total of 100 frames.

Imaging

All microscopy experiments were performed at 22°C. To image the localization of fluorescent proteins in cells, 10^5 cells were plated in an 8-well coverslip chamber (Lab-Tek; NalgenNunc) and allowed to adhere. Images were taken on a Zeiss 880 inverted microscope equipped with a 40×/0.95 or 63×/1.4 oil-immersion objective. To image GFP-Atg8a signal, cells were incubated in HL5 or submerged in DB for 1 h before imaging. For experiments presented in Fig. S5A, the HL5 medium was supplemented with 2.5× protease inhibitor cocktail (Roche 11836170001) under the plus PIC condition.

For experiments presented in Fig. 7C, cells were plated in an 8-well coverslip chamber and allowed to adhere. Before imaging, the medium was replaced by fresh HL5 medium containing 1 mg/ml FD. For experiments presented in Fig. S4, cells were incubated in HL5 medium containing 1 mg/ml FD and 500 µg/ml TD. FD and TD signals contained within the newly generated macropinosomes were quantified by ImageJ. The ratio of FD to TD was used to measure macropinosome acidification with the maximum ratio normalized to 1.

Quantification and statistical analysis

SuperPlots were generated as described previously (Lord et al., 2020). Statistical analysis was performed using GraphPad Prism. ***P<0.001, **P<0.01 and *P<0.05 (all figures).

Acknowledgements

We thank Dr Robert Kay (MRC Laboratory of Molecular Biology, UK) for providing Ax2, DdB, *pi3k1-5* null cells and pDM vectors; Dr Richard Firtel (University of California San Diego, US) for *pi3k1-2* null cells; Dr Xiaochen Wang (Institute of Biophysics, Chinese Academy of Sciences, China) for FYVE and TAPP1 plasmids; and Dr Jason King (University of Sheffield, UK) for RFP-VatB plasmid.

Competing interests
The authors declare no competing or financial interests.

Author contributions
Conceptualization: H.C.; Formal analysis: H.C., H.W., Y.Z., H.T., Z.G., L.L.; Investigation: Y.Z., H.T., H.W., Y.H., D.L., Y. Yang, Y. Yuan; Writing - original draft: H.C., H.W.; Writing - review & editing: H.C., H.W., Y.Z., H.T., L.L.; Supervision: H.C.; Project administration: H.C.; Funding acquisition: H.C., H.W., Y. Yang.

Funding
This work was supported by grants from the Ministry of Science and Technology of China (2021YFA1300301), the Strategic Priority Research Program of Chinese Academy of Sciences (XDB37020304), the National Natural Science Foundation of China (32170701, 32071232 and 31872828), and the Youth Innovation Promotion Association of Chinese Academy of Sciences (2020096).

Peer review history
The peer review history is available online at https://journals.biologists.com/jcs/article-lookup/doi/10.1242/jcs.259450.

References

Bloomfield, G., Traynor, D., Sander, S. P., Veltman, D. M., Pachebat, J. A. and Kay, R. R. (2015). Neurofibromin controls macropinocytosis and phagocytosis in Dictyostelium. *eLife* **4**, e04940. doi:10.7554/eLife.04940

Buckley, C. M. and King, J. S. (2017). Drinking problems: mechanisms of macropinosome formation and maturation. *FEBS J.* **284**, 3778-3790. doi:10.1111/febs.14115

Buckley, C. M., Pots, H., Gueho, A., Vines, J. H., Munn, C. J., Phillips, B. A., Gilsbach, B., Traynor, D., Nikolaev, A., Soldati, T. et al. (2020). Coordinated Ras and Rac activity shapes macropinocytic cups and enables phagocytosis of geometrically diverse bacteria. *Curr. Biol.* **30**, 2912-2926.e5. doi:10.1016/j.cub.2020.05.049

Charpentier, J. C., Chen, D., Lapinski, P. E., Turner, J., Grigorova, I., Swanson, J. A. and King, P. D. (2020). Macropinocytosis drives T cell growth by sustaining the activation of mTORC1. *Nat. Commun.* **11**, 180. doi:10.1038/s41467-019-13997-3

Clarke, M. and Kayman, S. C. (1987). Chapter 8 The axenic mutations and endocytosis in Dictyostelium. *Methods Cell Biol.* **28**, 157-176. doi:10.1016/S0091-679X(08)61642-8

Commisso, C., Davidson, S. M., Soydaner-Azeloglu, R. G., Parker, S. J., Kamphorst, J. J., Hackett, S., Grabocka, E., Nofal, M., Drebin, J. A., Thompson, C. B. et al. (2013). Macropinocytosis of protein is an amino acid supply route in Ras-transformed cells. *Nature* **497**, 633-637. doi:10.1038/nature12138

Condon, N. D., Heddleston, J. M., Chew, T.-L., Luo, L., McPherson, P. S., Ioannou, M. S., Hodgson, L., Stow, J. L. and Wall, A. A. (2018). Macropinosome formation by tent pole ruffling in macrophages. *J. Cell Biol.* **217**, 3873-3885. doi:10.1083/jcb.201804137

Daniel, H., Spanier, B., Kottra, G. and Weitz, D. (2006). From bacteria to man: archaic proton-dependent peptide transporters at work. *Physiology* **21**, 93-102. doi:10.1152/physiol.00054.2005

Donaldson, J. G. (2019). Macropinosome formation, maturation and membrane recycling: lessons from clathrin-independent endosomal membrane systems. *Philos. Trans. R. Soc. Lond B. Biol. Sci.* **374**, 20180148. doi:10.1098/rstb.2018.0148

Dormann, D., Weijer, G., Dowler, S. and Weijer, C. J. (2004). In vivo analysis of 3-phosphoinositide dynamics during Dictyostelium phagocytosis and chemotaxis. *J. Cell Sci.* **117**, 6497-6509. doi:10.1242/jcs.01579

Egami, Y., Taguchi, T., Maekawa, M., Arai, H. and Araki, N. (2014). Small GTPases and phosphoinositides in the regulatory mechanisms of macropinosome formation and maturation. *Front Physiol.* **5**, 374. doi:10.3389/fphys.2014.00374

Faix, J., Kreppel, L., Shaulsky, G., Schleicher, M. and Kimmel, A. R. (2004). A rapid and efficient method to generate multiple gene disruptions in Dictyostelium discoideum using a single selectable marker and the Cre-loxP system. *Nucleic Acids Res.* **32**, e143. doi:10.1093/nar/gnh136

Freeman, S. A., Uderhardt, S., Saric, A., Collins, R. F., Buckley, C. M., Mylvaganam, S., Boroumand, P., Plumb, J., Germain, R. N., Ren, D. J. et al. (2020). Lipid-gated monovalent ion fluxes regulate endocytic traffic and support immune surveillance. *Science* **367**, 301-305. doi:10.1126/science.aaw9544

Fujii, M., Kawai, K., Egami, Y. and Araki, N. (2013). Dissecting the roles of Rac1 activation and deactivation in macropinocytosis using microscopic photo-manipulation. *Sci. Rep.* **3**, 2385. doi:10.1038/srep02385

Hacker, U., Albrecht, R. and Maniak, M. (1997). Fluid-phase uptake by macropinocytosis in Dictyostelium. *J. Cell Sci.* **110**, 105-112. doi:10.1242/jcs.110.2.105

Hoeller, O., Bolourani, P., Clark, J., Stephens, L. R., Hawkins, P. T., Weiner, O. D., Weeks, G. and Kay, R. R. (2013). Two distinct functions for PI3-kinases in macropinocytosis. *J. Cell Sci.* **126**, 4296-4307. doi:10.1242/jcs.134015

Ito, K., Hikida, A., Kawai, S., Lan, V. T., Motoyama, T., Kitagawa, S., Yoshikawa, Y., Kato, R. and Kawarasaki, Y. (2013). Analysing the substrate multispecificity of a proton-coupled oligopeptide transporter using a dipeptide library. *Nat. Commun.* **4**, 2502. doi:10.1038/ncomms3502

Junemann, A., Filić, V., Winterhoff, M., Nordholz, B., Litschko, C., Schwellenbach, H., Stephan, T., Weber, I. and Faix, J. (2016). A Diaphanous-related formin links Ras signaling directly to actin assembly in macropinocytosis and phagocytosis. *Proc. Natl. Acad. Sci. USA.* **113**, E7464-E7473. doi:10.1073/pnas.1611024113

Kayman, S. C. and Clarke, M. (1983). Relationship between axenic growth of Dictyostelium discoideum strains and their track morphology on substrates coated with gold particles. *J. Cell Biol.* **97**, 1001-1010. doi:10.1083/jcb.97.4.1001

Keim, M., Williams, R. S. B. and Harwood, A. J. (2004). An inverse PCR technique to rapidly isolate the flanking DNA of dictyostelium insertion mutants. *Mol. Biotechnol.* **26**, 221-224. doi:10.1385/MB:26:3:221

Kim, S. M., Nguyen, T. T., Ravi, A., Kubiniok, P., Finicle, B. T., Jayashankar, V., Malacrida, L., Hou, J., Robertson, J., Gao, D. et al. (2018). PTEN deficiency and AMPK activation promote nutrient scavenging and anabolism in prostate cancer cells. *Cancer Discov.* **8**, 866-883. doi:10.1158/2159-8290.CD-17-1215

King, J. S. and Kay, R. R. (2019). The origins and evolution of macropinocytosis. *Philos. Trans. R. Soc. Lond. B Biol. Sci.* **374**, 20180158. doi:10.1098/rstb.2018.0158

King, J. S., Veltman, D. M. and Insall, R. H. (2011). The induction of autophagy by mechanical stress. *Autophagy* **7**, 1490-1499. doi:10.4161/auto.7.12.17924

King, B., Araki, J., Palm, W. and Thompson, C. B. (2020). Yap/Taz promote the scavenging of extracellular nutrients through macropinocytosis. *Genes Dev.* **34**, 1345-1358. doi:10.1101/gad.340661.120

Kuspa, A. (2006). Restriction enzyme-mediated integration (REMI) mutagenesis. *Methods Mol. Biol.* **346**, 201-209. doi:10.1385/1-59745-144-4:201

Lee, S.-W., Zhang, Y., Jung, M., Cruz, N., Alas, B. and Commisso, C. (2019). EGFR-Pak signaling selectively regulates glutamine deprivation-induced macropinocytosis. *Dev. Cell* **50**, 381-392.e5. doi:10.1016/j.devcel.2019.05.043

Li, W., Zou, W., Zhao, D., Yan, J., Zhu, Z., Lu, J. and Wang, X. (2009). C. elegans Rab GTPase activating protein TBC-2 promotes cell corpse degradation by regulating the small GTPase RAB-5. *Development* **136**, 2445-2455. doi:10.1242/dev.035949

Lin, X. P., Mintern, J. D. and Gleeson, P. A. (2020). Macropinocytosis in different cell types: similarities and differences. *Membranes* **10**, 177. doi:10.3390/membranes10080177

Lord, S. J., Velle, K. B., Mullins, R. D. and Fritz-Laylin, L. K. (2020). SuperPlots: communicating reproducibility and variability in cell biology. *J. Cell Biol.* **219**, e202001064. doi:10.1083/jcb.202001064

Maekawa, M., Terasaka, S., Mochizuki, Y., Kawai, K., Ikeda, Y., Araki, N., Skolnik, E. Y., Taguchi, T. and Arai, H. (2014). Sequential breakdown of 3-phosphorylated phosphoinositides is essential for the completion of macropinocytosis. *Proc. Natl. Acad. Sci. USA.* **111**, E978-E987. doi:10.1073/pnas.1311029111

Mylvaganam, S., Freeman, S. A. and Grinstein, S. (2021). The cytoskeleton in phagocytosis and macropinocytosis. *Curr. Biol.* **31**, R619-R632. doi:10.1016/j.cub.2021.01.036

Norbury, C. C., Hewlett, L. J., Prescott, A. R., Shastri, N. and Watts, C. (1995). Class I MHC presentation of exogenous soluble antigen via macropinocytosis in bone marrow macrophages. *Immunity* **3**, 783-791. doi:10.1016/1074-7613(95)90067-5

Palm, W. (2019). Metabolic functions of macropinocytosis. *Philos. Trans. R. Soc. Lond. B Biol. Sci.* **374**. 20180285. doi:10.1098/rstb.2018.0285

Palm, W., Park, Y., Wright, K., Pavlova, N. N., Tuveson, D. A. and Thompson, C. B. (2015). The utilization of extracellular proteins as nutrients is suppressed by mTORC1. *Cell* **162**, 259-270. doi:10.1016/j.cell.2015.06.017

Palm, W., Araki, J., King, B., DeMatteo, R. G. and Thompson, C. B. (2017). Critical role for PI3-kinase in regulating the use of proteins as an amino acid source. *Proc. Natl. Acad. Sci. USA.* **114**, E8628-E8636. doi:10.1073/pnas.1712726114

Paschke, P., Knecht, D. A., Silale, A., Traynor, D., Williams, T. D., Thomason, P. A., Insall, R. H., Chubb, J. R., Kay, R. R. and Veltman, D. M. (2018). Rapid and efficient genetic engineering of both wild type and axenic strains of Dictyostelium discoideum. *PLoS ONE* **13**, e0196809. doi:10.1371/journal.pone.0196809

Ramirez, C., Hauser, A. D., Vucic, E. A. and Bar-Sagi, D. (2019). Plasma membrane V-ATPase controls oncogenic RAS-induced macropinocytosis. *Nature* **576**, 477-481. doi:10.1038/s41586-019-1831-x

Rivero, F. and Maniak, M. (2006). Quantitative and microscopic methods for studying the endocytic pathway. *Methods Mol. Biol.* **346**, 423-438. doi:10.1385/1-59745-144-4:423

Rosel, D., Khurana, T., Majithia, A., Huang, X., Bhandari, R. and Kimmel, A. R. (2012). TOR complex 2 (TORC2) in Dictyostelium suppresses phagocytic nutrient

capture independently of TORC1-mediated nutrient sensing. *J. Cell Sci.* **125**, 37-48. doi:10.1242/jcs.077040

Rupper, A., Lee, K., Knecht, D. and Cardelli, J. (2001). Sequential activities of phosphoinositide 3-kinase, PKB/Aakt, and Rab7 during macropinosome formation in Dictyostelium. *Mol. Biol. Cell* **12**, 2813-2824. doi:10.1091/mbc.12.9.2813

Sallusto, F., Cella, M., Danieli, C. and Lanzavecchia, A. (1995). Dendritic cells use macropinocytosis and the mannose receptor to concentrate macromolecules in the major histocompatibility complex class II compartment: downregulation by cytokines and bacterial products. *J. Exp. Med.* **182**, 389-400. doi:10.1084/jem.182.2.389

Sattler, N., Bosmani, C., Barisch, C., Gueho, A., Gopaldass, N., Dias, M., Leuba, F., Bruckert, F., Cosson, P. and Soldati, T. (2018). Functions of the Dictyostelium LIMP-2 and CD36 homologues in bacteria uptake, phagolysosome biogenesis and host cell defence. *J. Cell Sci.* **131**, jcs218040. doi:10.1242/jcs.218040

Shao, X., Cao, G., Chen, D., Liu, J., Yu, B., Liu, M., Li, Y.-X., Cao, B., Sadovsky, Y. and Wang, Y.-L. (2021). Placental trophoblast syncytialization potentiates macropinocytosis via mTOR signaling to adapt to reduced amino acid supply. *Proc. Natl. Acad. Sci. USA.* **118**, e2017092118. doi:10.1073/pnas.2017092118

Shaulsky, G., Escalante, R. and Loomis, W. F. (1996). Developmental signal transduction pathways uncovered by genetic suppressors. *Proc. Natl. Acad. Sci. USA.* **93**, 15260-15265. doi:10.1073/pnas.93.26.15260

Smith, D. E., Clémençon, B. and Hediger, M. A. (2013). Proton-coupled oligopeptide transporter family SLC15: physiological, pharmacological and pathological implications. *Mol. Asp. Med.* **34**, 323-336. doi:10.1016/j.mam.2012.11.003

Steel, A., Nussberger, S., Romero, M. F., Boron, W. F., Boyd, C. A. and Hediger, M. A. (1997). Stoichiometry and pH dependence of the rabbit proton-dependent oligopeptide transporter PepT1. *J. Physiol.* **498**, 563-569. doi:10.1113/jphysiol.1997.sp021883

Swanson, J. A. (2014). Phosphoinositides and engulfment. *Cell. Microbiol.* **16**, 1473-1483. doi:10.1111/cmi.12334

Terada, T., Irie, M., Okuda, M. and Inui, K.-I. (2004). Genetic variant Arg57His in human H+/peptide cotransporter 2 causes a complete loss of transport function. *Biochem. Biophys. Res. Commun.* **316**, 416-420. doi:10.1016/j.bbrc.2004.02.063

Veltman, D. M., Akar, G., Bosgraaf, L. and Van Haastert, P. J. M. (2009). A new set of small, extrachromosomal expression vectors for Dictyostelium discoideum. *Plasmid* **61**, 110-118. doi:10.1016/j.plasmid.2008.11.003

Veltman, D. M., Lemieux, M. G., Knecht, D. A. and Insall, R. H. (2014). PIP3-dependent macropinocytosis is incompatible with chemotaxis. *J. Cell Biol.* **204**, 497-505. doi:10.1083/jcb.201309081

Veltman, D. M., Williams, T. D., Bloomfield, G., Chen, B.-C., Betzig, E., Insall, R. H. and Kay, R. R. (2016). A plasma membrane template for macropinocytic cups. *eLife* **5**. e20085. doi:10.7554/eLife.20085

Verdon, Q., Boonen, M., Ribes, C., Jadot, M., Gasnier, B. and Sagné, C. (2017). SNAT7 is the primary lysosomal glutamine exporter required for extracellular protein-dependent growth of cancer cells. *Proc. Natl. Acad. Sci. USA.* **114**, E3602-E3611. doi:10.1073/pnas.1617066114

Williams, T. D. and Kay, R. R. (2018). The physiological regulation of macropinocytosis during Dictyostelium growth and development. *J. Cell Sci.* **131**, jcs213736. doi:10.1242/jcs.213736

Wolfson, R. L. and Sabatini, D. M. (2017). The Dawn of the age of amino acid sensors for the mTORC1 pathway. *Cell Metab.* **26**, 301-309. doi:10.1016/j.cmet.2017.07.001

Wyant, G. A., Abu-Remaileh, M., Wolfson, R. L., Chen, W. W., Freinkman, E., Danai, L. V., Vander Heiden, M. G. and Sabatini, D. M. (2017). mTORC1 activator SLC38A9 is required to efflux essential amino acids from lysosomes and use protein as a nutrient. *Cell* **171**, 642-654.e12. doi:10.1016/j.cell.2017.09.046

Xu, L., Haworth, I. S., Kulkarni, A. A., Bolger, M. B. and Davies, D. L. (2009). Mutagenesis and cysteine scanning of transmembrane domain 10 of the human dipeptide transporter. *Pharm. Res.* **26**, 2358-2366. doi:10.1007/s11095-009-9952-9

Yao, W., Rose, J. L., Wang, W., Seth, S., Jiang, H., Taguchi, A., Liu, J., Yan, L., Kapoor, A., Hou, P. et al. (2019). Syndecan 1 is a critical mediator of macropinocytosis in pancreatic cancer. *Nature* **568**, 410-414. doi:10.1038/s41586-019-1062-1

Yoshida, S., Hoppe, A. D., Araki, N. and Swanson, J. A. (2009). Sequential signaling in plasma-membrane domains during macropinosome formation in macrophages. *J. Cell Sci.* **122**, 3250-3261. doi:10.1242/jcs.053207